Crystallographic and Magnetic Properties of $CuRh_2Se_4$ – $FeRh_2Se_4$ Series

Chul Sung Kim (金哲聖) and In Bo Shim
Departments of Physics, Kookmin University, Seoul, 136-702, R.O.K.

(Received Jan. 20, 1990)

The mixed series $CuRh_2Se_4$ – $FeRh_2Se_4$ has been synthesized and studied by x-ray, Mossbauer, and magnetic measurements at temperatures between 4.2 and 300 K. We found that the crystal structure of $Fe_xCu_{1-x}Rh_2Se_4$ is transformed from spinel to monoclinec structure as iron concentration increases. The isomer shift measurements indicated that the charge state of the Fe ions undergoes gradual change from ferric to ferrous iron as x is increased. The origin of this transition seems to be in the-change of ionic radius of iron ions from smaller one of Fe^{3+} to large one of Fe^{2+}. All the samples become antiferromagnets. $FeRh_2Se_4$ has been synthesized and the crystal structure is found to be monoclinic with the lattice parameter: a = 6.310 Å, b = 3.643 Å, c = 11.14 Å, β = 92.42°. The structure is characterized by ordered vacancies in alternate metal layers. The iron ions are found to be ferrous in charge state and occupy the metal layers which are without vacancies, which is "inverse" to the site distributions reported for similar structures.

I. INTRODUCTION

The magnetic and crystallographic properties of $CuRh_2Se_4$ are well known. The compound $CuRh_2Se_4$ crystallizes with a normal spinel structure[1] of lattice parameter a = 10.259 Å in which the Cu ions occupy the tetrahedral(A) sites, and Rh ions the octahedral(B) sites. The valence state of the Rh ions is trivalent and, because the crystal field is large,[2] they are in the low-spin ground state t_{2g}^6. $CuRh_2Se_4$ shows a temperature independent paramagentism with a molar susceptibility of (0.5-1.1) X 10^{-4} emu/mole at liquid nitrogen temperature, which has been concluded to be mainly due to Van Vleck paramagnetism.[3] In the past twenty years, a number of attempts[4-7] have been made to prepare the ternary-compound series of rhodium, $FeRh_2X_4$ (X = O, S, Se, Te), but they have failed to yield single-phase products. Blasse[4] expended considerable efforts in vain to synthesize $FeRh_2O_4$ and speculated that the state of (Fe^{3+} + Rh) is more stable than that of (Fe^{2+} + Rh^{3+}). Recently, another attempt was made by Spencer et al.[6] which also ended in failure. Similar failures have been reported for $FeRh_2S_4$.[5] $FeRh_2Se_4$ and $FeRh_2Te_4$[7] despite many variations in the preparation conditions.

The purpose of this study is to carry out Mossbauer and magnetic susceptibility

measurements on the series $Fe_xCu_{1-x}Rh$, Se, to study magnetic interactions exclusively on the A site. This is possible because all the B sites are occupied by the diamagnetic Rh^{3+} ions.

II. EXPERIMENTALS

Synthesis of the $Fe_xCu_{1-x}Rh_2$ Se, samples was accomplished by direct-reaction of the elements in an evacuated quartz tube. The starting materials were high-purity Fe (99.995%) Cu (99.999%), Rh (99.99%) and Se (99.999%). Mixtures of the elements in the proper proportions were sealed in evacuated quartz ampoules and heated at 500 °C for two days, at 700 °C for two days, at 1050 °C for three days, at 1080 °C for 10 hours and then slowly cooled to room temperature at a rate of 1 0°C/h. In order to obtain a homogeneous material, it was necessary to grind the samples after the first firing and to press the powders into pellets before annealing them for a second time in evacuated and sealed quartz ampoules. In most instances, a third firing similar to the second one was required. The samples were partially enriched in ^{57}Fe (5 at.%) to facilitate Mossbauer measurements.

X-ray diffraction patterns of the samples were obtained using a Norelco diffractometer with Cu K_α radiation. A slow scanning speed, i.e., 0.25" advance in 2θ per min., was used in order to optimize resolution of the closely spaced reflections. Mossbauer spectra were recorded using a conventional Mossbauer spectrometer of the electromechanical type* with a ^{57}Co source in a rhodium matrix. To produce a uniform thickness over the area of the Mossbauer absorber, each sample was mixed with boron nitride powder and clamped between two thin boron nitride plates.

The magnetization and susceptibility of the samples at temperatures between 5 and 300 K were measured with a SQUID (Superconducting Quantum Interference Device) magnetometer manufactured by the S.H.E. Corporation.

III. RESULTS AND DISCUSSION

III-1 Crystal structure and site distribution

Figure 1. shows X-ray diffraction patterns for $Fe_xCu_{1-x}Rh_2$ Se, (x = 0.1, 0.7, 1.0) at room temperature. X-ray diffraction patterns of the samples showed that the samples with composition in the range of $0 \leqslant x \leqslant 0.3$ had the spine1 structure. The lattice parameter, a, for each composition was found by plotting $a(\theta)$ against the Nelson-Riley function' and extrapolating to $\theta = 90"$. The value of a increases with increasing iron concentration x. On the other hand, as x increased to 0.4, a monoclinic phase appears and it is no longer possible to prepare a single-phase spine1 structure. Every peak in the pattern can be indexed on a monoclinic cell for $FeRh_2$ Se, (x = 1 .O). All observed reflections satisfy the condition h+k+l = 2n (n = integer), indicating a body-centered unit cell. Cell parameters were calculated and refined using a computer program of a least-squares method. The resulting

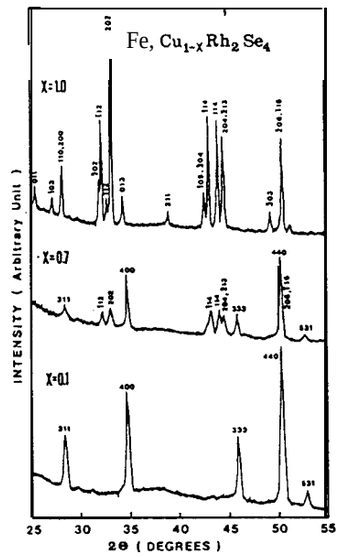

FIG. 1. X-ray diffraction patterns of $Fe_xCu_{1-x}Rh_2Se_4$ at room temperature. Horizontal Miller indices indicate spinel structure, whereas vertical indices indicate monoclinic structure.

cell parameters[10] are found to be a = 6.310 ± 0.005 A, b = 3.643 ± 0.003 A, c = 11.14 ± 0.01 A and β = 92.42 ± 0.05 A. Since the lattice is body-centered, a plausible structure is the following:"

(0,0,0 ; ½, ½, ½) +

2 A in (O,V,O) with V ~ 0

4 B in (U,V,W; –U,V,–W) with U ~ 0, V ~ 0, W ~ ¼.

4 Se in (U,V,W; –U,V,–W) with U ~ $^1/_3$, V ~ 0, W ~ $^3/_8$.

4 Se in (U,V,W; -U,V,-W) with U ~ $^1/_3$, V ~ 0, W ~ $^7/_8$.

Figure 2. shows this defect Ni-As structure in which the A-sites are in the layers with ordered vacancies, and the B-sites in the layers without vacancies. In order to find out how

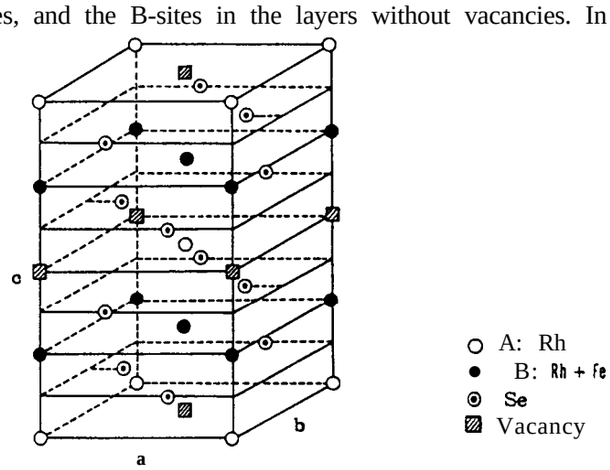

FIG. 2. The metal substructure of the monoclinic defect Ni – As structure of Fe Rh_2 Se,.

two Fe and Four Rh ions in a unit cell are distributed among the A-and B-sites, the observed diffraction intensities are compared with the following three models.

Model (1) All the A-sites are occupied by Fe ions, while all the B-sites are occupied by Rh ions.

Model (2) One half of the Fe ions occupy A-sites and the other half of the Fe ions, occupy B-sites; all the other A-and B-sites are occupied by Rh ions.

Model (3) All the A-sites are occupied by Rh ions, while one half of the B-sites have Fe ions and the other half Rh ions.

We have calculated the diffraction intensities for each model and compared them with the observed intensities. For comparison, a disagreement factor, defined by $R = \Sigma |I_{obs.} - I_{calc.}| / \Sigma I_{obs}$, was calculated. In this calculation we have neglected small displacements of the ions from the above ideal positions. For convenience of calculation, analytical expressions[12] for the atomic scattering factors were used together with anomalous dispersion corrections[13] for all ions. The calculation shows that the R factors are 0.43, 0.28, and 0.23 for models (1),(2), and (3), respectively. From this result, model (1) is ruled out, and model (3) is a little better than model (2). However, the Mossbauer spectra of $FeRh_2$ Se,, as shown in the next section, show that only one kind of site is occupied by the Fe^{+2} ions, thereby excluding model (2). Therefore, model (3) was adopted and further refinements of the least-squares calculation carried out allowing small displacements from the ideal positions. The results of the calculation are shown in Table I along with the observed

TABLE I. Calculated and observed diffraction intensities for $FeRh_2$ Se,. R = 0.12 was obtained from this calculation.

h,k,l	$I_{calc.}$		$I_{obs.}$	h,k,l	$I_{calc.}$		$I_{obs.}$
iol	19.3	25.5	31	ii4	64.5		64
002	6.2			114	72.3		76
101	27.5		23	204	22.4		25
011	15.8		10	$\bar{2}13$	19.1		27
$\bar{1}03$	10.3		6	$\bar{3}03$	6.9		12
110	13.2	30.4	30	310	69.7	102.0	98
200	17.2			020	32.3		
202	28.4		32	$\bar{2}06$	6.9		5
ii2	98.6		100	$\bar{1}16$	6.9		7
112	27.0		23	116	12.9		14
202	51.5		51	$\bar{1}07$	6.4		8
013	23.5		21	$\bar{2}22$	5.5		8
211	9.9		11	222	19.4		12
$\bar{2}04$	26.8	27.3	29	008	12.1		23
$\bar{1}05$	0.5			224	7.2		14

intensities. The final structure shown in Table II suggests that the space group is 12. Finally, it should be noted that the site distributions in the pseudo-hexagonal monoclinic $FeRh_2Se_4$

TABLE II. Atomic positions in the monoclinic unit cell of $FeRh_2$ Se,. B. C. indicates a body - centered position.

Ions	Positions	U	V	W
2 Rh^{3+}	0, V, 0; B.C.		0.053	
2 Rh^{3+}, 2 Fe^{2+}	U,V,W; –U,V,–W; B.C.	-0.023	-0.035	0.259
2 Se	U,V,W; –U,V,–W; B.C.	0.347	-0.05 1	0.368
2 Se	U,V,W; -U,V,-W; B.C.	0.349	-0.008	0.886

are "inverted", namely $A^{3+}B^{3+}B^{2+}X_4$, which is in marked contrast with the "normal" distribution, $A^{2+}B_2{}^{3+}X_4$, so far observed in all other pseudo-hexagonal monoclinic structures such as MRh_2X_4 (M = Cr, Co, Ni; X = Se, Te),[7] MTi_2X_4 (M = Fe, Co, Ni; X = S, Se),[14] and NiM_2X_4 (M = Cr, V; X = S, Se)."

III-2 Mossbauer and magnetic measurements

Mossbauer spectra were measured for all the spine1 samples at various absorber temperatures from 4.2 K to room temperature. Spectra below the magnetic ordering temperature T_N were fitted to six Lorentzians while those above T_N were fitted to a single Lorentzian.

Figures 3. and 4. show some of the Mossbauer spectra of $Fe_xCu_{1-x}Rh_2$ Se, at room temperature. As can be seen in these figures, the spectra for the composition range x ≤ 0.3 exhibit a single absorption line with no observable quadrupole splitting. The isonier shift

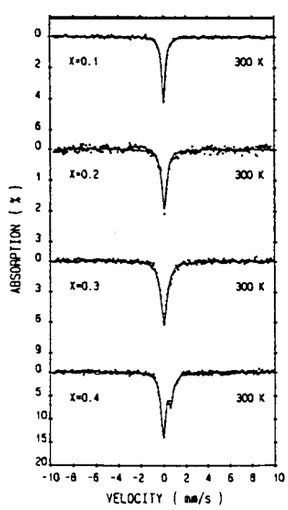

FIG. 3. Mossbauer spectra of Fe, $Cu_{1-x}Rh_2Se_4$ at room temperature (I).

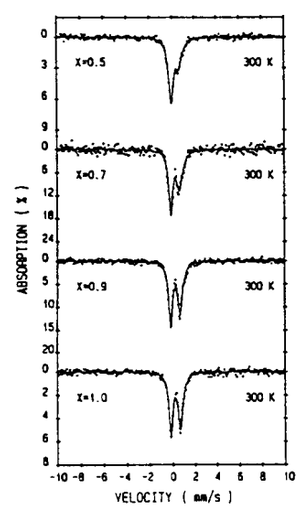

FIG. 4. Mossbauer spectra of $Fe_xCu_{1-x}Rh_2Se_4$ at room temperature (II).

with respect to iron metal is 0.42 ± 0.01 mm/s, independent of composition in the spine1

phase ($x \leqslant 0.3$). This value of isomer shift indicates that the charge state of Fe ions in the spinel phase is ferric.[16] However, as x is increased to 0.4, a monoclinic phase appears and it is no longer possible to prepare a single absorption line. The absence of quadrupole splitting in the spinel phase in both paramagnetic and magnetically ordered states is consistent with the expectation that the A-sites are occupied by iron ions because the local symmetry of the A-site is cubic T_d while that of the B-site is trigonal D_{3d}.[17]

Figure 5. show the Mossbauer spectra of $Fe_xCu_{1-x}Rh_2Se$, (x = 0.1, 0.3, 1.0) at 4.2 K. The results of the analysis, shown in Table III, establish that the effective magnetic field H_{eff} increases with increasing iron concentration (x).

TABLE III. Isomer shift (IS), quadrupole splitting (QS), effective hyperfine field (H_{eff}) of Fe, $Cu_{1-x}Rh_2Se$, at 4.2 K.

x	IS (mm/sec)	QS (mm/sec)	H_{eff} (kOe)
0.1	0.42	0.008	142
0.3	0.43	0.015	174
1.0	0.66	1.03	175

We have taken Mossbauer spectra of the monoclinic structure of $FeRh_2Se$, at various absorber temperatures from 4.2 to 762 K. The spectra consist of quadrupole doublet with a high-temperature linewidith of 0.30 mm/s; some of them are shown in Figs. 4,5 and 6. The isomer shift at room temperature is 0.66 ± 0.01 mm/s relative to Fe metal, which means that the charge state of the Fe ion has a ferrous character.[18] As can be seen in Fig. 6. Mossbauer lines are asymmetric for $FeRh_2Se$,. This kind of asymmetry can be ascribed to

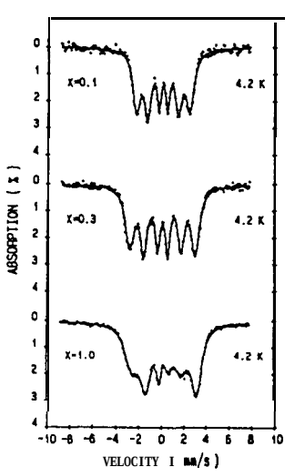

FIG. 5. Mossbauer spectra of $Fe_xCu_{1-x}Rh_2Se_4$ at 4.2 K.

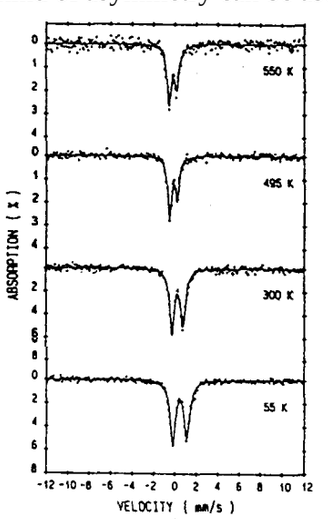

FIG. 6. Mossbauer spectra of $FeRh_2Se_4$.

the Goldanskii-Karyagin effect, relaxation effect, and texture." The third effect, related to the preferred orientation of crystallites, was eliminated by using finely powdered samples. To distinguish between the first two effects, it is necessary to observe temperature dependence of the asymmetry. Since the asymmetry increases with increasing temperature as shown in Fig. 6, it is due to the Goldanskii-Karyagin effect.[19,20]

The isomer shift at room temperature is plotted as a function of the iron concentration in Fig. 7. Values characteristic for Fe^{3+} ions change gradual by to those typical for Fe^{+2} ions as x is increased from 0.4 towards 1 .O. Fig. 8. shows reduced hyperfine field as a function of reduced temperature for Fe, $_3Cu_{0.7}Rh_2Se_4$. Solid curve is the Brillouin function for S =5/2. The gyperfine field indicates that the Fe ions are in a high-spin state with S=5/2.

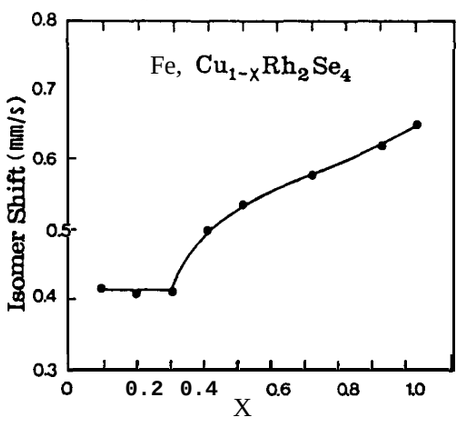

FIG. 7. Compositional dependence of the isomer shift of $Fe_xCu_{1-x}Rh_2Se_4$.

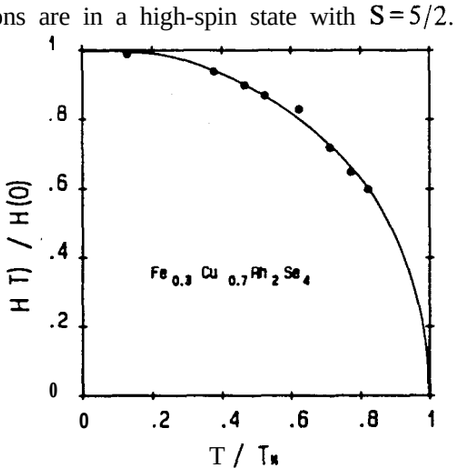

FIG. 8. Reduced hyperfine field as a function of reduced temperature for $Fe_{0.3}Cu_{0.7}Rh_2Se_4$. Solid curve is the Brillouin function for S= 5/2.

Now we are going to justify the exclusion of the model (2) for $FeRh_2$ Se, in the preceding section. In the defect Ni-As structure, both A- and B-sites are surrounded octahedrally by six nearest-neighbor Se ions at a distance of 2.5 A as shown in Fig. 9. However, each A-site ion is coordinated closely with two next-nearest-neighbor B-site ions at a distance of 2.8 Å whereas each B-site ion is coordinated with only one A-site ion at the same distance. Furthermore, each B-site ion is surrounded hexagonally by six third-nearest-neighbor B-site ions at a distance of 3.6 A on a hexagonal basal plane while each A-site ion by only two A-site ions at the same distance. In view of such a large difference between the local atomic arrangements of A- and B-sites, it is improbable that ferrous ions at both A- and B-sites show not only the same magnitude but also the temperature dependence of quadrupole splittings over the wide temperature range from 55-762 K. Therefore it may by concluded that only one kind of site, namely a B-site, is occupied by Fe^{2+} ions.

The quadrupole splitting is 1.04 mm/s at 55 K and decreases rapidly with increasing temperature as shown in Fig. 10. Since the Fe^{2+} in $FeRh_2$ Se, is surrounded octahedrally by six neighboring Se ions and is also in an axial crystal field due to approximately hex-

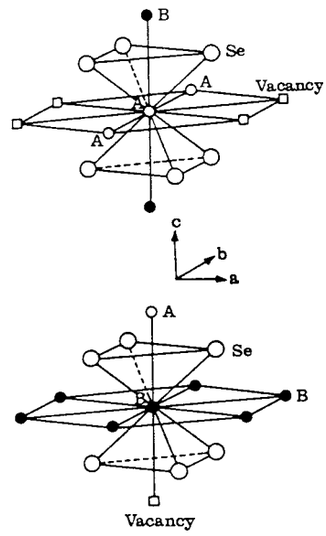

FIG. 9. Local atomic arrangements of A and B sites in the defect Ni – As structure.

agonal crystal symmetry, the temperature dependence of the quadrupole splitting could be analyzed in terms of the thermal populations of the finely split levels of the $d\epsilon$ state using Ingalls's method.[21]

However, his method is limited for $FeRh_2$ Se, due to the highly covalent nature of the Fe-Se bonding as will be shown below. Application of this method to quadrupole splittings below 300 K gave the following results:[22] the $d\epsilon$ level splits into a singlet and a

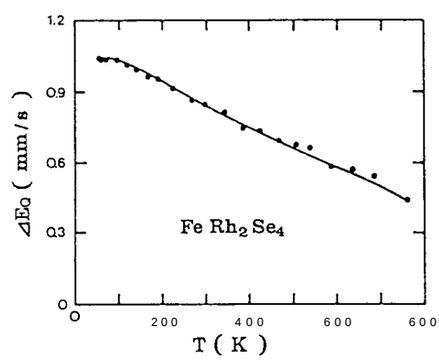

FIG. 10. Temperature dependence of the quadrupole splitting.

doublet, with the doublet at a lower energy than the singlet by an energy separation of 2.7λ (λ = the magnitude of the spin-orbit coupling constant for ^5D of Fe^{2+}). According to the quadrupole-splitting-isomer -shift correlation in octahedral iron compounds,[23] the isomer shift of 0.66 mm/s and the normalized quadrupole splitting of 2 x 1.04 mm/s for the doublet ground state mean that $FeRh_2$ Se, is a covalent compound, and $\langle r^{-3} \rangle$ takes a small value of about 2.3 a.u. due to the radial expansion of the $3d(t_{2g})$, wave function.

The temperature dependence of the susceptibility of $Fe_{0.3}Cu_{0.7}Rh_2Se_4$ and $FeRh_2$ Se,

under an applied field H_a = 8kG and 990 G, respectively, are shown in Figs. 11. and 12. in both zero-field-cooled (ZFC) and field-cooled (FC) modes. Above T_N, the FC and ZFC data are nearly identical. Below T_N, the ZFC and FC data are totally different. The cusp-

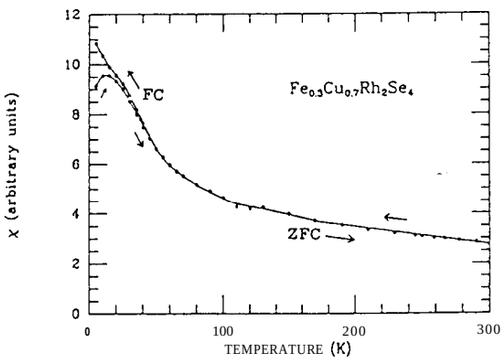

FIG. 1 1. Typical zero-field-cooled and field-cooled magnetic suscpetibility vs temperature curves with an applied field of H_a=8 KG.

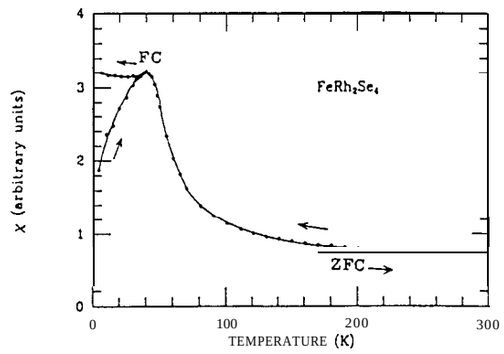

FIG. 12. Typical zero-field-cooled and field-cooled magnetic susceptibility vs temperature curves with an applied of Ha = 990 G.

like behavior of the ZFC data, and the difference between FC and ZFC results are very similar to those found in the antiferromagnetic state.[24] The results for $FeRh_2$ Se, with several applied fields (H, = 20, 103 and 990 G) are shown in Fig. 13. It is noted that the value of T_N is well defined and not sensitive to the magnitude of the low applied DC field. For larger fields, the cusp is smoothed into a broadened peak.

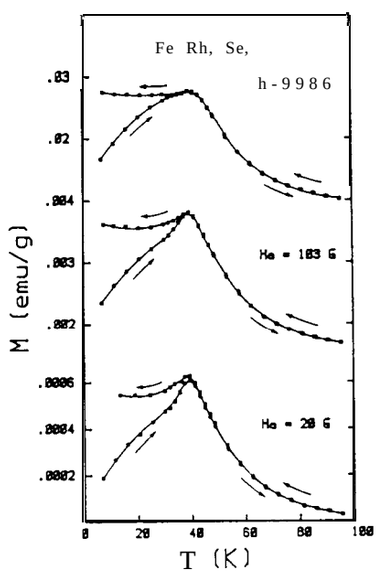

FIG. 13. Temperature dependence of the zero-field-cooled and field-cooled magnetization of $FeRh_2$ Se, with various applied fields (Ha =20, 103,990 G).

The temperature dependence of the high temperature magnetic susceptibility χ for most of the samples can be well described by the Curie-Weiss relation:

$$\chi = \frac{C}{T-\Theta} = \frac{N_A g^2 J(J+1)\mu_B^2}{3k_B(T-\Theta)}$$

where C is the Curie constant, Θ is the paramagnetic Curie temperature, N_A is Avogadro's number, gis the Lande g-factor, J is the value of the total spin, μ_B is the Bohr magneton, and k_B is Boltzmann's constant.

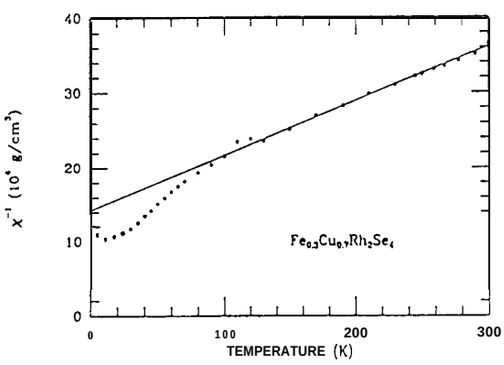

FIG. 14. Reciprocal of the magnetic susceptibility as a function of temperature for $Fe_{0.3}Cu_{0.7}Rh_2Se_4$.

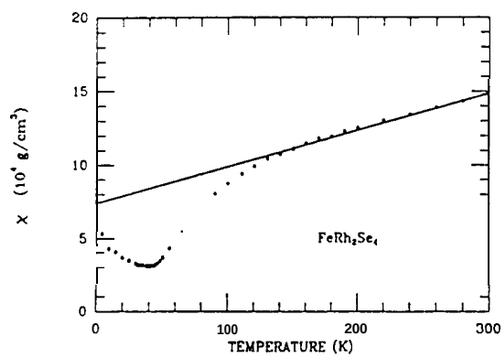

FIG. 15. Reciprocal of the magnetic susceptibility as a function of temperature for $FeRh_2$ Se,.

Typical inverse-susceptibility versus T curves are shown in Figs. 14. and 15. and Table IV lists the experimental molar Curie constant C_M (C_M = Curie constant x mole weight) and the paramagnetic Curie temperature Θ obtained from the measurements along with the Curie constants calculated using the spin-only values of the ferric and ferrous ions. From Table IV, we see that the molar Curie constant C_M increases with x, reflecting the fact that C_M is proportional to the concentration of magnetic ions. However, the values of C_M are

TABLE IV. The compositional dependence of the molar Curie constant C_M, the paramagnetic Curie temperature Θ, the spin-only molar Curie constant $C_{M'}$, and the Neel temperature T_N for $Fe_x Cu_{1-x} Rh_2$ Se,

x	C_M (emu/mole)	Θ (K)	C', (emu/mole)	C_M/C'_M	T_N (K)
0.1	0.29	-120	0.44	0.66	10
0.3	0.74	-165	1.31	0.57	15
1.0	1.99	-194	3.01	0.66	40

much smaller than the values of the theoretical spin-only molar Curie constants $C_{M'}$. Similar reductions have been reported for $CoRh_2S_4$,[25] $CuFeS_2$[26] and MCo_2O_4 (m = Mn, Fe,

Co, Ni).[27] Qualitatively, we may explain this reduction in terms of a participation of the 3d (t_{2g}) electrons of iron in the covalent bonding.

Table IV also shows that the values of Θ are negative, thereby suggesting that the superexchange interaction between iron ions is antiferromagnetic. Among possible exchange mechanisms a direct exchange between the A-sits is improbable the A-A distance in the spinel structure is $\frac{1}{4}\sqrt{3}\,a$; for a = 10.271 Å in $Fe_{0.3}Cu_{0.7}$ Rh, Se,, the A-A distance is 4.447 Å which seems too large to give rise to any direct interaction of importance. A superexchange of Fe^{3+}-Se-Fe^{3+} is also improbable, because the A-Se distances for the A-Se-A bond are $1/8\sqrt{3}$ a and $1/8\sqrt{11}$ a (where the selenium parameter u = 3/8); for a = 10.271 Å these are 2.224 and 4.259 A, respectively. However, there are three kinds of long distance interactions in which separations between two neighboring ions are within 2.6 A. Blasse[4,28] proposed an interaction of the type Fe – Se – Rh^{3+} – Se – Fe indicated by (a) in Fig. 16. and Plumier and Lotgering[29] two kinds of interactions, Fe – Se – Rh^{3+} – Se – Fe and Fe – Se – Rh^{3+} – Se – Rh^{3+} – Se – Fe, indicated by (b) and (c), respectively, in Fig. 16. In

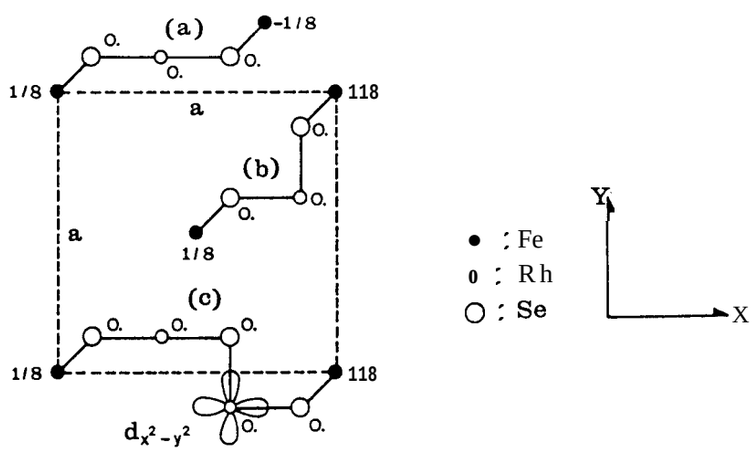

FIG. 16. Three kinds of long-distance superexchange interactions of the spinel phase for $Fe_xCu_{1-x}Rh_2Se_4$. z-coordinates of the ions are given in fractional units of a.

these configurations the Fe – Se and Se – Rh distances are $1/8\sqrt{3}$ a and a/4, respectively; thus for a = 10.271 A, these are only 2.224 and 2.568 A respectively, thereby allowing for interactions of reasonable strength. The Fe-Se-Rh band angle is about 125" but the Se-Rh-Se angles are either 90" or 180" as shown in Fig. 16. Since Rh^{3+} in the spinel structure has low-lying empty e_g orbitals ($d_{x^2-y^2}$, d_{z^2}), it seems likely that both the 90" and 180" Se – Rh – Se superexchange interactions are similar in magnitude. Among possible exchange mechanisms a direct exchange for monoclinic $FeRh_2$ Se, is of minor importance because the Fe^{2+} – Fe^{2+} distance is as large as 3.643 A. A 90" superexchange of Fe^{2+} – Se^{-2} – Fe^{2+} seems to be responsible for the antiferromagnetic exchange mechanism, the Fe – Se distances for Fe – Se – Fe are 2.47 and 2.55 Å respectively; the Fe – Se – Fe bond angle is 93".

Figure 17. shows the magnetization curves at 5 K for $Fe_{0.3}Cu_{0.7}$ Rh, Se, and $FeRh_2Se_4$

with magnetic fields varing between zero and 50 kG. Themagnetization curves behave linearly to the applied field. From the magnetization curves, we conclude that $Fe_{0.3}Cu_{0.7}Rh_2$ Se, and $FeRh_2$ Se, are purely antiferromagnetic compounds.[30]

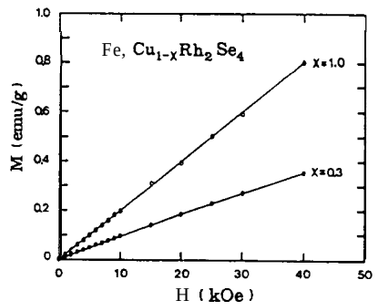

FIG. 17. Magnetization curvs at T = 5 K for $Fe_xCu_{1-x}Rh_2Se_4$.

ACKNOWLEDGMENTS

This work was supported by the Korea Science and Engineering Foundation.

REFERENCES

1. M. Robbins, H. W. Lehmann, and J. G. White, J. Phys. Chem. Solids 28,897 (1967).
2. J. B. Goodenough, J. Phys. Chem. Solids **30**, 26 1 (1969).
3. H. N. Ok, K. S. Baek and C. S. Kim, Phys. Rev. B 25, 7034 (1982); F. K. Lotgering and R. P. van Stapele, J. Appl. Phys. 39, 417 (1968); C. S. Kim, K. S. Baek and H. N. Ok, New Physics (Korea) 22, 125 (1982).
4. G. Blasse, Philips Res. Rep. 18, 383 (1963); Philips Tech. Rev. 28, 23 (1967).
5. C. Boumford and A. H. Morrish, Phys. Rev. B 17, 1323 (1978).
6. C. D. Spencer, P. A. Smith, C. M. Karnes and W. A. Shepard, J. Phys. Chem. Solids 41, 1079 (1980).
7. R. H. Plovnick and A. Wold, Inorg. Chem. 7, 2596 (1968).
8. C. S. Kim, I. B. Shim, H. S. Lee, and C. S. Kim, New Physics (Korea) 29, 772 (1989).
9. J. B. Nelson and D. P. Riley, Proc. Phys. Soc. 7, 160 (1945).
10. H. N. Ok, K. S. Baek and C. S. Kim, Phys. Rev. B **26**, 4436 (1982).
11. F. Jellinek, Acta Cryst. 10, 620 (1957).
12. D. T. Cromer and J. B. Mann, Acta Cryst. A 24, 321 (1968).
13. D. T. Cromer, Acta Cryst. 18, 17 (1965).
14. R. H. Plovinck, M. Vlasse, and A. Wold, Inorg. Chem. 7, 127 (1968).
15. R. J. Bouchard and A. Wold, J. Phys. Chem. Solids 27, 591 (1966).
16. R. Ingalls, F. van der Woude and G. A. Sawatzky in ***Mossbauer Isomer Shifts,*** edited by F. K. Sheony and F. E. Wager (North-Holland Publ. Co., Amsterdam, 1978); M. R.

Spender, J. M. D. Coey and A. H. Morrish, Can. J. Phys. 50, 23 13 (1972).
17. C. S. Kim, J. Childress, and C. L. Chien, J. Appl. Phys. 64, 5886 (1988).
18. H. K. Ok and S. W. Lee, Phys. Rev. B 8, 4267 (1973); C. S. Kim, S. K. Jeong, J. Y. Park, and H. N. Ok, J. Korean Phys. Soc. 22, 363 (1989).
19. J. J. Spijkermann, F. C. Ruegg, and L. May, in ***Mossbauer Effect Methodology,*** edited by I. J. Gruverman (Plenum, New York, 1966), Vol. 2, p. 854.
20. H. A. Stockler and H. Sano, in ***Mossbauer Effect Methodology,*** edited by I. J. Gruverman (Plenum, New York, 1970), Vol. 5, p. 3.
21. R. Ingalls, Phys. Rev. 133, A 787 (1964).
22. H. N. Ok, K. S. Baek, and C. S. Kim, New Physics (Korea) 22, 250 (1982).
23. Y. Hazony, in ***Mossbauer Effect Methodology,*** edited by I. J. Gruverman (Plenum, New York, 1971), Vol. 7, p. 147.
24. A. H. Morrish, The ***Physical Principles of Magnetism,*** (John Wiley & Sons, Inc., New York, 1965) p. 461.
25. F. K. Lotgering, J. Phys. Chem. Solids 30, 1429 (1969).
26. G. Donnay, L. M. Corliss, J. D. H. Donnay, N. Elliot, and J. M. Hastings, Phys. Rev. 112, 1917 (1958); H. N. Ok and C. S. Kim, Nuovo Cimento **28B**, 138 (1975).
27. F. K. Lotgering, Philips Res. Rep. **11**, ***337 (1956).***
28. Blasse, Phys. Lett. 19, 110 (1965).
29. R. Plumier and F. K. Lotgering, Solid State Commun. 8, 477 (1970); H. N. Ok, K. S. Baek, and C. S. Kim, New Physics (Korea) 22, 1369 (1982).
30. G. Blasse and J. F. Fast, Philips Res. 18, 393 (1963).